J Intell Robot Syst (2011) 61:29–42
DOI 10.1007/s10846-010-9480-1

Vision Based Control for Fixed Wing UAVs Inspecting Locally Linear Infrastructure Using Skid-to-Turn Maneuvers

Steven J. Mills · Jason J. Ford · Luis Mejías

Received: 1 February 2010 / Accepted: 1 September 2010 / Published online: 28 October 2010

Abstract The following paper proposes a novel application of Skid-to-Turn maneuvers for fixed wing Unmanned Aerial Vehicles (UAVs) inspecting locally linear infrastructure. Fixed wing UAVs, following the design of manned aircraft, commonly employ Bank-to-Turn maneuvers to change heading and thus direction of travel. Whilst effective, banking an aircraft during the inspection of ground based features hinders data collection, with body fixed sensors angled away from the direction of turn and a panning motion induced through roll rate that can reduce data quality. By adopting Skid-to-Turn maneuvers, the aircraft can change heading whilst maintaining wings level flight, thus allowing body fixed sensors to maintain a downward facing orientation. An Image-Based Visual Servo controller is developed to directly control the position of features as captured by onboard inspection sensors. This improves on the indirect approach taken by other tracking controllers where a course over ground directly above the feature is assumed to capture it centered in the field of view. Performance of the proposed controller is compared against that of a Bank-to-Turn tracking controller driven by GPS derived cross track error in a simulation environment developed to replicate the field of view of a body fixed camera.

Keywords Skid-to-Turn · Image based visual servoing · Guidance and control · Fixed wing UAVs

This work was conducted within the CRC for Spatial Information, established and supported under the Australian Government's Cooperative Research Centres Programme.

S. J. Mills · J. J. Ford · L. Mejías (✉)
Australian Research Centre for Aerospace Automation (ARCAA),
Queensland University of Technology (QUT), Brisbane, QLD, 4001, Australia
e-mail: luis.mejias@qut.edu.au

S. J. Mills
e-mail: sj.mills@qut.edu.au

J. J. Ford
e-mail: j2.ford@qut.edu.au

1 Introduction

Recent years have seen a steady increase in the use of Unmanned Aerial Vehicles (UAVs) in civilian applications, particularly those involving inspection and surveillance [1, 8]. Fixed wing platforms are used in many of these roles given their endurance, range and payload capabilities, however are faced with a challenge when attempting to track linear features as the platform is unable to generate a direct lateral force to correct for cross track error. Over the past two decades a number of controller designs have come forth seeking to address this issue, minimizing the time taken to acquire a desired track [4, 9].

Commonly overlooked however, is the effect maneuvers have on the inspection process. Even though in many instances the primary objective of the UAV is to collect data over a target, focus falls to the design of a controller that can reduce the time to converge with a track over the feature, inevitably leading to the use of aggressive roll rates and step bank angles. These maneuvers however hinder the data collection process, reducing data quality and potentially causing features to leave the Field of View (FOV) of sensors. Even once steady state conditions have been reached and the desired track acquired, steady state pitch and roll angles can see features offset in the sensor FOV. Of the research that does recognize the problem, solutions can be grouped under one of two approaches; decoupling of body and sensor motion through the use of a gimballed sensor mount and through the limitation of aircraft motion.

Stolle and Rysdyk develop an algorithm that generates path guidance and synchronous angle commands for a pan and tilt camera to observe ground based targets [11, 12]. A disadvantage however with gimballed cameras is the limited range of motion and thus compensation available for use, a point which is acknowledged by the authors and addressed through maneuvers that maximize target exposure. Holt and Beard also employ a gimballed camera, however present a proportional navigation solution based on a Skid-to-Turn (STT) kinematic model mapped to a Bank-to-Turn (BTT) Miniature Aerial Vehicle (MAV) with a single axis gimballed camera [5]. Although both solutions address the problem at hand, the integration of a gimballed sensor mount is far from trivial and would be avoided if possible. Reducing the motion that causes the problems is one such solution.

Egbert and Beard take this approach and introduce roll constraints given the altitude of the BTT MAV in an attempt to maintain the footprint of the body fixed camera over a pathway [3]. Although an effective solution for BTT only MAV and UAVs, it introduces an unwanted trade-off between altitude and turn radius. In addition, the effect of roll rate on sensors is not addressed which could lead to issues with data quality. Rathinam et al. take a vision based approach to the tracking problem, using feature extraction to locate and update the ground coordinates of the feature being tracked [10]. Although this allows for on the fly adjustments to the flight plan, correcting for position errors that may see gross errors within captured data, no compensation is made for the effect of maneuvers on the inspection process.

The following paper proposes a novel use of Skid-to-Turn (STT) maneuvers for fixed wing UAVs inspecting locally linear infrastructure. Through simulation, it is shown that by adopting such maneuvers unwanted motion can be reduced whilst maintaining the feature of interest in the FOV of downward facing, body fixed sensors. An Image-Based Visual Servo (IBVS) controller is developed to track

features directly from the image plane of a downward facing camera, thus re-focusing the guidance and control problem on the inspection task at hand. FOV Track Error is proposed as a performance metric to replace Cross Track Error, which is shown to inaccurately capture the behavior of tracking controllers when used for inspection. The proposed controller is evaluated against that of a postion based, lateral track controller employing Bank-to-Turn maneuvers following a simulated powerline corridor.

The paper is structured as follows. Section 2 details the step by step design of the IBVS controller and how STT maneuvers are managed. Section 3 introduces the simulation environment and test cases developed to test the performance of the proposed controller and how images were generated to simulate the downward facing camera. Section 4 then presents the outcome of simulation tests and discusses findings. Finally, a short summary concludes the paper, with discussion of future work.

2 Problem Formulation

The conventional means of altering the heading of a fixed wing aircraft is through a Bank-to-Turn (BTT) maneuver. By rolling the aircraft about the longitudinal axis and inducing a bank angle, the resultant lift vector produces the necessary horizontal force to turn. Given the magnitude of the lift vector and angle of bank achievable, a considerable amount of turning force can be generated. This does however have a significant impact on those sensors mounted orthogonal to the longitudinal axis (i.e., downward facing cameras), which are now subjected to a panning motion that can not only induce motion blur, but angles the sensor away from the direction of turn.

Alternatively, Skid-to-Turn (STT) maneuvers can be used to change heading, yawing the aircraft to produce a sideslip angle, β, between the longitudinal axis and relative airflow. The resultant thrust vector produces a component of force perpendicular to the relative airflow and coupled with additional aerodynamic force created by the now exposed fuselage and vertical stabilizers, allows the aircraft to change heading. As rotation is only required about the yaw axis, the aircraft can maintain wings level flight during the maneuver, thus allowing sensors to maintain their FOV [14].

STT maneuvers do however have their disadvantages, particularly with larger manned aircraft, hence their limited use. Whilst flying in a sideslip, the fuselage is exposed to the relative airflow which leads to increased drag and reduced efficiency, while the lateral acceleration experienced by passengers can cause discomfort. The amount of turning force that can be generated is also limited and dependent on the inherent directional stability of the platform which restricts the maximum β angle the aircraft can maintain. For these reasons the use of STT maneuvers in aviation are generally restricted to cross wind landings and aerobatics.

Any number of control techniques can be used in conjunction with STT maneuvers to improve data collection. In this instance visual servo control has been chosen to track features directly within the image plane. Originally developed to control serial-link robotic manipulators fitted with cameras mounted on end effectors, two variations of control arose, namely Position-Based Visual Servoing (PBVS) and

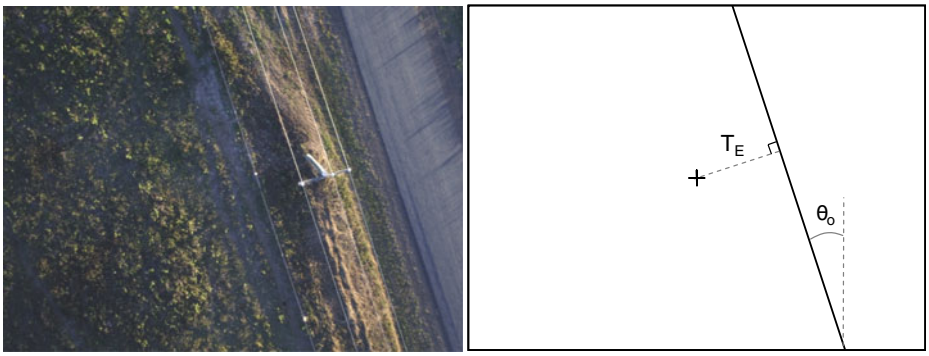

Fig. 1 Representation of linear features identified in the image plane through the use of track error, T_e, and observed line angle, θ_o

Image-Based Visual Servoing (IBVS) [2]. While PBVS reconstructs the pose of the object with respect to the camera, IBVS uses error measurements taken directly from the image plane between the observed and desired pose of image features. IBVS is chosen in this instance as reliance on accurate camera pose and intrinsic camera parameters can be avoided, of which accurate data may not be available [6].

Identifying suitable features for tracking is essential and considering the case of locally linear infrastructure, the feature can be modeled as a straight line within the image plane. Figure 1 illustrates this with a section of powerline imaged from a low flying UAV (approx. 100 ft) where the feature has been modeled by a single straight line and its position and orientation defined by track error, T_e, and observed line angle, θ_o. This approach can be used to model any infrastructure once appropriate feature extraction algorithms have been applied. For the purpose of this paper, it is assumed that images have been preprocessed.

Ideally the feature is to remain centered in the FOV for the duration of the inspection process, which from a control perspective implies driving T_e to zero and flying at a ground track[1] angle equal to the features orientation with respect to Earth. It should be noted that this does not imply the aircraft maintains a ground track over the feature, as steady state pitch and roll angles may require the aircraft to fly slightly off center for the feature to be centered in the FOV. Considering the case where the aircraft is operating in no wind and sensor alignment is with the body axis, the feature can be expected to run vertically through the image plane, or more specifically, the observed line angle, θ_o, would be zero. Thus in this instance the controller seeks to drive T_e and θ_o to zero. This however only applies to the ideal situation where the aircraft operates in no wind.

When introduced to wind, the aircraft's heading and track over ground become separated by a drift angle, or wind correction angle (WCA) as it is sometimes termed when the aircraft course is adjusted to compensate for wind. This angle between

[1] *Ground Track* is also sometimes referred to as *Course over Ground*.

body fixed and inertial coordinate frames translates through to the camera frame and under steady state conditions will see the observed line pass diagonally through the image center, with an observed line angle, θ_o, equal to WCA. Although weather predictions and ground track from GPS can provide an estimate of WCA, ideally the IBVS controller will compensate with no prior knowledge.

Having identified control features and their desired pose, the next step in development looks at how STT maneuvers can control pose. Although minimizing track error is the primary focus, T_e alone provides insufficient information to account for current approach angle, which is critical for rapid convergence and limited overshoot. This research proposes the use of T_e to derive a desired line angle, θ_d, that once established, will set the UAV on a trajectory that minimizes T_e. Figure 2 illustrates

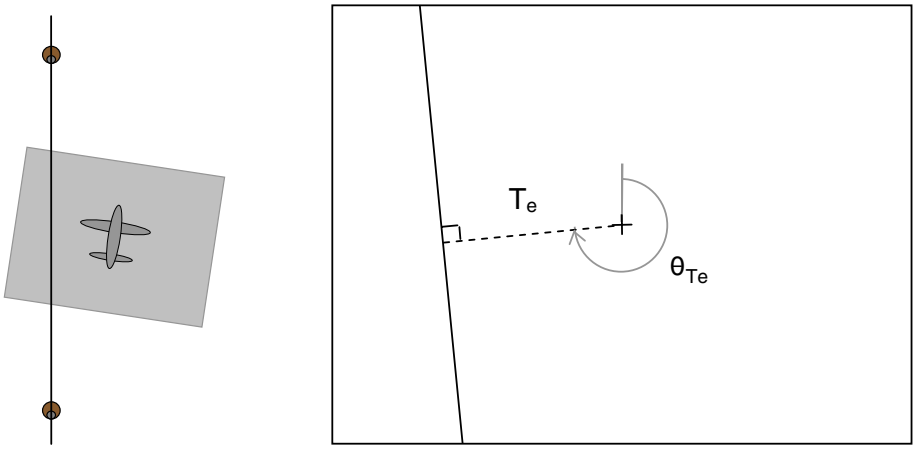

(a) View of aircraft and feature from above (*left*) and image plane (*right*)

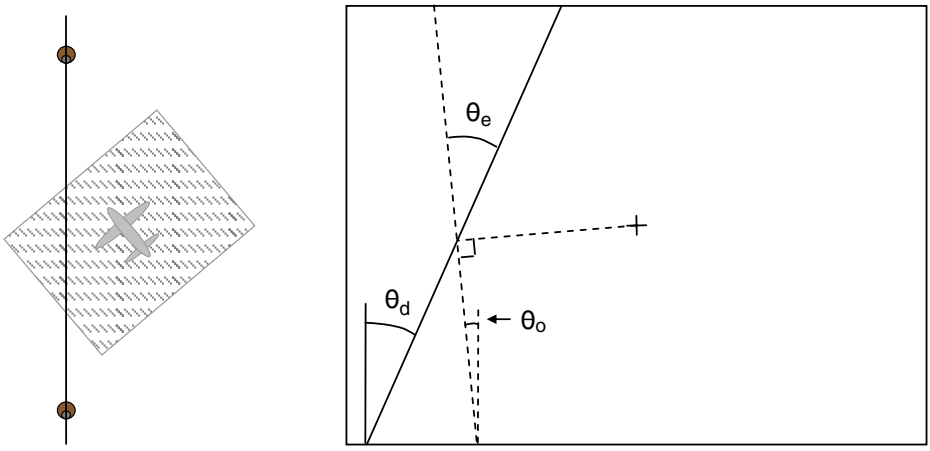

(b) Desired heading and line angle as would be seen from above (*left*) and in the image plane (*right*)

Fig. 2 Establishing desired line angle, θ_d, from track error, T_e, as observed in the image plane

this with an example of an aircraft flying, wings level, over a powerline attempting to maintain it centered in the FOV.

Figure 2a shows the initial position of the aircraft and a simulated image as would be captured by a downward facing camera. From the image one can infer the aircraft is right of the feature and flying away, based on θ_o. To bring the feature towards the center of the image, the aircraft itself must also move towards the feature, requiring a heading similar to that depicted in Fig. 2b. This would see the feature captured as the solid line, referred to as the desired line angle, θ_d, for which the controller must drive the aircraft towards. This however forms but one case and if extended for all values of T_e produces a relationship similar to that of Fig. 3a. Note, the sign of T_e defines the lines position as being in the left or right half of the image plane, or more specifically, the angle with respect to the vertical θ_{Te}, as shown in Fig. 2a, defines $+T_e$ for the right half of the image plane for angles between 0 and π and $-T_e$ for angles between π and 2π for the left half. $+\theta_d$ refers to the line angle measured clockwise over 0 to π, while $-\theta_d$ is measured from 0 to $-\pi$. When tracked over time the aircraft can be expected to follow a path similar to that shown in Fig. 3b.

Mathematically, the curve shown in Fig. 3a can be described by the sigmoid function,

$$f(T_e) = \frac{\pi}{\left(1 + e^{\frac{T_e}{k_s}}\right)} - \frac{\pi}{2} \tag{1}$$

where k_s defines the slope of the function through the transition and thus can be used to adjust the rate at which the aircraft approaches the target. Desired angle can then be expressed as follows with the inclusion of residual track error and approach velocity feedback for wind conditions,

$$\theta_d = \frac{\pi}{\left(1 + e^{\frac{T_e}{k_s}}\right)} - \frac{\pi}{2} + V_a + R_{Te} \tag{2}$$

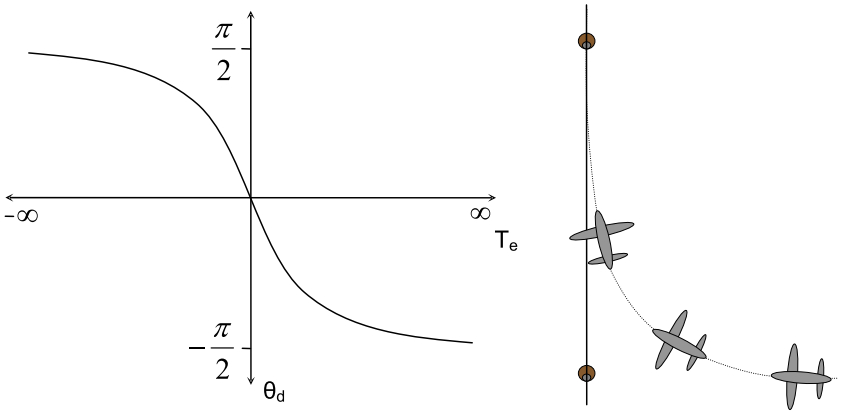

(a) Desired Angle versus Track Error (b) Desired Trajectory

Fig. 3 A sigmoid relationship between track error and desired line angle is adopted to generate a converging trajectory

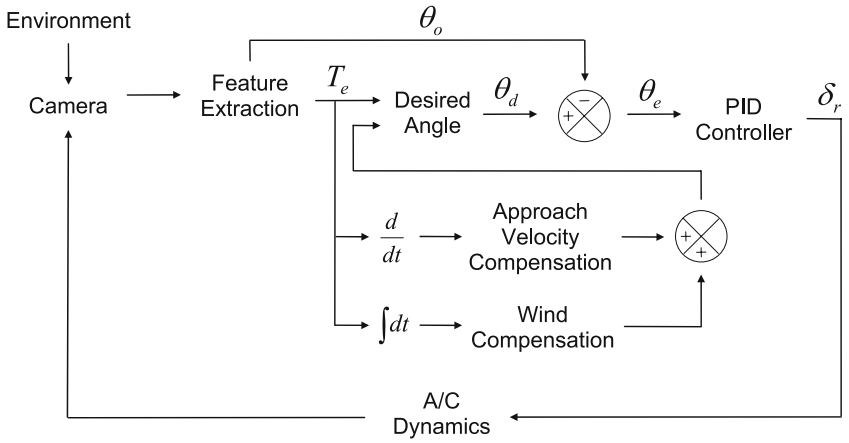

Fig. 4 System Diagram of Skid-to-Turn Image-Based Visual Servo control scheme

where V_a, the compensation for approach velocity and R_{Te}, compensation for residual track error, are expressed as follows,

$$V_a = k_v \frac{dT_e}{dt} \tag{3}$$

$$R_{Te} = k_r \int T_e \, dt \tag{4}$$

Maneuvering the aircraft so that θ_o equals θ_d is achieved through rudder deflections generated by a PID controller driven by angle error, θ_e, given as,

$$\theta_e = \theta_d - \theta_o \tag{5}$$

Under this design, ailerons and elevators are free to operate independently of the IBVS controller and thus can be used to maintain altitude and hold wings level. In this way, a conventional autopilot can be used to navigate the aircraft to the inspection site, where the IBVS controller can then take over control of the rudder, issuing commands to the autopilot to maintain altitude and wings level. Figure 4 illustrates the control architecture.

3 Experiment

To test the performance of the STT IBVS controller, a simulation environment was developed upon Matlab Simulink that could replicate the FOV of a body fixed, downward facing, image sensor. To generate images, the location of turning points in the simulated linear infrastructure where transformed from Earth Centered Earth Fixed (ECEF) coordinates to camera image plane coordinates through a series of standard photogrammetric transforms [7, 13]. Connecting turning points within the camera image plane, T_e and θ_o could then be estimated and used as input to the

IBVS controller. The response of the aircraft to rudder commands generated by the controller are then simulated using a nonlinear, 6 degrees of freedom, dynamic model of an Aerosonde UAV, which in turn provides the state variables required for ECEF to image plane coordinate transformations. Separate controllers were developed to maintain airspeed, altitude and wings level, emulating an autopilot that would operate independent of the IBVS controller.

To compare the performance of the proposed controller to that of a conventional BTT controller, a GPS driven lateral track controller was implemented. Although many controller options exist in this area, the use of BTT maneuvers is common throughout and subsequently the behaviour on sensor FOV is expected to be reflected by all. The controller implemented in this instance reduces cross track error through a continuous adjustment of heading calculated as follows;

$$\phi_d = \phi_f + \frac{\pi}{2} - \frac{\pi}{\left(1 + e^{\frac{C_{Te}}{k_s^*}}\right)} \tag{6}$$

where ϕ_d is desired bearing, ϕ_f bearing of the feature, C_{Te} cross track error and k_s^* the approach rate similar to that of k_s in Eq. 1. In this instance k_s^* varies to compensate for the velocity at which the aircraft is approaching the line and modifies k_s in the following manner;

$$k_s^* = k_s + k_v \left(\frac{dC_{Te}}{dt} - v_d\right) \tag{7}$$

where k_v and v_d are both constant and control the amount of velocity compensation and desired approach velocity respectively. For this experiment controller gains k_s, k_v, v_d were set to 20, 2 and 5, respectively and remained constant over the course of all simulations.

A series of scenarios were then developed to test the performance of the controllers under typical operating conditions. Powerline inspection is used as an example to set real world parameters, modeling a three wire distribution line with 20 m easements and 10 m poles spaced at 100 m. Initially the aircraft is positioned off to one side of the line, flying parallel, from which position it must maneuver back over the line. Corners and bends are not considered at this stage. Flight parameters including autopilot gains, desired altitude and airspeed are all held constant for the duration of each scenario. Selection of altitude during these missions is highly dependent on camera parameters, with angular FOV and spatial resolution limiting the lower and upper limits respectively. The camera model used in this instance has a 50° horizontal angular FOV and a resolution of 1,024 × 768 pixels, effectively limiting the lower altitude at which the aircraft can fly and still capture the full corridor to 50 m, while the ability to see the lines limiting the highest altitude to approximately 100 m.

Airspeed selection is less constrained, with lower speeds favored to avoid motion blur and increase image overlap, with higher speeds favored to increase efficiency and range. With respect to the Aerosonde, the slowest speed at which the aircraft can still maintain altitude is approximately 70 km/h, while increased efficiency can be achieved around 100 km/h. The final test condition would introduce wind, and whilst

initial tests would be performed under no wind conditions, subsequent tests would introduce a worst case scenario of a direct cross wind acting across the powerlines, in this instance a 15 kt (7.7 m/s) wind. Test cases would then be developed to test the full combination of height, airspeed and wind, bounding the expected working conditions of the system. After initial tuning, IBVS controller gains k_s, k_v and k_r, where set to 300, 0.1 and 0.035, respectively and would remain constant for all scenarios, as would be required in practice.

4 Results

Parameters for the first series of tests were selected to reflect ideal operating conditions, no wind and altitude and airspeed set to 50 m and 70 km/h, respectively. To evaluate and compare performance, two metrics, Track Error and FOV Track Error, were introduced, both providing a relative measure of aircraft position with respect to the feature. Track Error in this instance refers to cross track error, the perpendicular distance from the aircraft to course over ground defined by the features centerline and is a common performance metric for lateral track controllers. FOV Track Error on the other hand, previously referred to as track error, T_e, provides a measure of the features position in the image plane. It should be noted that the two controllers tested are not directly comparable in that the BTT based controller seeks to reduce GPS derived track error whilst the STT IBVS controller seeks to minimize FOV Track Error. This is however useful to highlight the general perception of lateral track controllers and the typical approach to design.

Initially the aircraft is positioned 15 m east of a line running north-south, a distance chosen to ensure the feature begins within the sensor FOV. The aircraft begins at the southern end of the line, heading north, thus the line appears on the left of the aircraft. Results for the first test, performed under no wind, are shown in Fig. 5. Track Error and FOV Track Error in this instance are on the y axis for better comparison, however it should be noted that the aircrafts direction of travel is interpreted left to right.

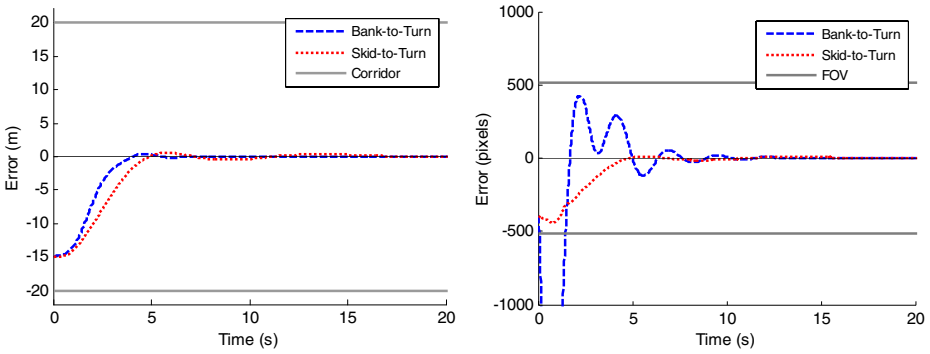

(a) Track Error with respect to feature centerline (b) Track Error as measured in the image plane

Fig. 5 Performance of Bank-to-Turn versus Skid-to-Turn controllers under ideal operating conditions (no wind, 70 km/h, at 50 m altitude)

As would be expected, the BTT controller performs well in re-positioning the aircraft over the line, with faster convergence and less overshoot than the STT controller. Traditionally this result would favor the use of the BTT controller, what is not considered though, is the impact on sensor FOV. Plotting FOV Track Error, as shown in Fig. 5b, it becomes clear the effect roll has on the image plane. Immediately the bank required to change heading results in the sensor pointing away from the feature, in this instance, at a sufficient angle to loose sight of the feature. As the plane levels out, the feature comes back within the FOV, only to then swing away again as the aircraft attempts to align with the feature. At this point the bank has a positive effect on the image plane, pointing the sensor towards the feature while it has yet to cross the line. Finally a small series of oscillations are seen as the aircraft reaches steady state. Another issue, not immediately obvious from Fig. 5b, is the rapid movement of features in the image plane, evident by the rate at which FOV Track Error changes, which would very likely result in motion blur during those frames.

Considering now the STT controller, it can be seen that a more desirable response is seen from the point of view of the image plane. Momentarily the feature moves away from the centre, caused by a sudden increase in lift on one wing as the aircraft begins to sideslip that takes the bank controller a moment to counteract. From this point on, FOV Track Error is slowly minimized and the feature is brought into the centre of the image with minimal overshoot or oscillations.

Although the STT controller displays better performance than the BTT controller in this scenario, a critical factor not considered is the effect of wind. Wind is a particular challenge for the IBVS controller as inertial data is not available for use and must be compensated for based on the features response within the FOV. Worst case scenario is in the presense of a direct cross wind with respect to the feature, or more specifically wind acting perpendicular to the feature. This can have two effects depending on the approach of the aircraft, with the aircraft either flying into the wind or with the wind as it re-positions over the line. To test both scenarios, a moderate wind of 15 kt (7.7 m/s) was applied from *west* to *east*, to test flying into the wind, and *east* to *west*, flying with the wind.

Figure 6a and b show the response of the aircraft flying into the wind to correct for position while Fig. 6c and d show the response as the aircraft flies with the wind. *Arrows* in each graph depict the direction of wind. As we would expect given no actual feedback for track error with respect to the feature centerline is provided to the STT IBVS controller, the response to re-positioning the aircraft over the line is far from ideal, while BTT has almost an identical response in both scenarios to that with no wind. However the effect on the image plane is quite clear, where the STT controller once again produces a far more desirable response. With the aircraft flying into the wind, Fig. 6a and b, the desired angle calculated by the STT controller to re-center the feature actually sees the aircraft draw short of the feature, creating a residual FOV Track Error that is slowly reduced over a period of 10 s.

A similar effect is seen with the aircraft flying with the wind, Fig. 6c and d, although in this instance the desired line angle generated by the IBVS controller causes the aircraft to overshoot before compensation for wind can be made. In this situation, velocity compensation plays a major role in slowing the rate of convergence, and thus avoiding overshoot. An interesting result of the BTT controller is seen after it reaches steady state, where the feature is slightly off center in both instances, an issue

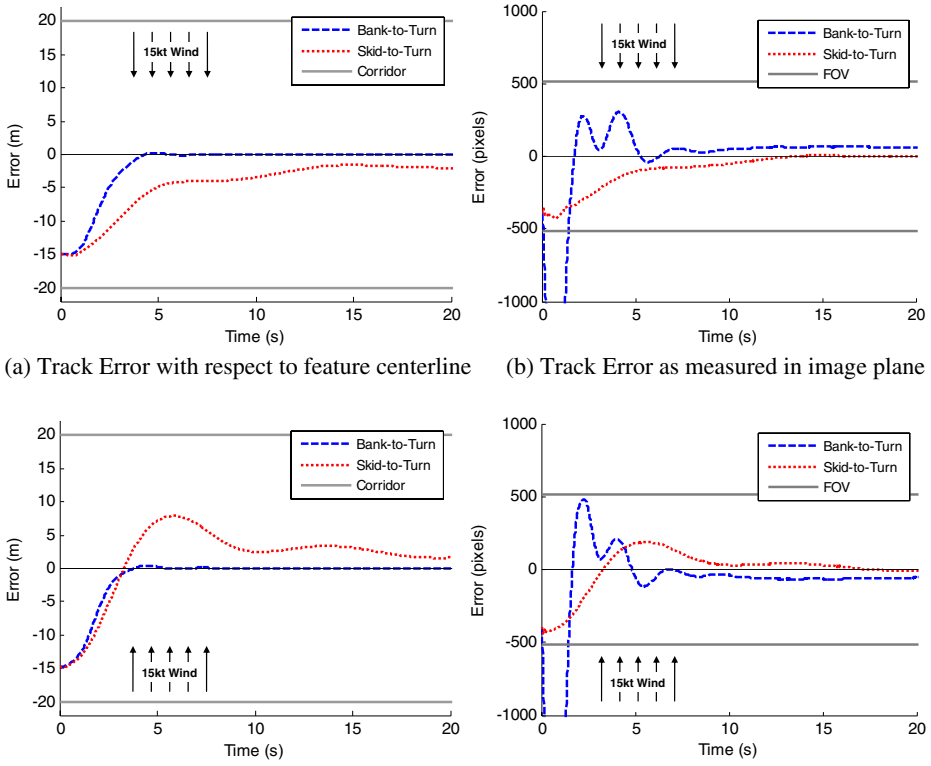

(a) Track Error with respect to feature centerline (b) Track Error as measured in image plane

(c) Track Error with respect to feature centerline (d) Track Error as measured in image plane

Fig. 6 Performance of tracking controllers in the presense of a 15 kt (7.7 m/s) cross wind. Aircraft flying into wind to re-position (**a**, **b**) and aircraft flying with the wind to re-position (**c**, **d**). Aircraft direction of travel is left to right, while *arrows* indicate direction of wind (70 km/h, 50 m altitude)

not observed during the initial scenario with no wind. This can be put down to pitch required to maintain altitude, which due to the WCA means the aircraft flies with a heading offset from track, thus pointing the sensor away from the line, instead of further along the line for the case of no wind. It can be seen from Fig. 6a and c that the IBVS controller accounted for this by maintaining steady state Track Error.

Having established that the controller can handle wind conditions, test scenarios were then introduced to evaluate the controller's response to changes in flight parameters. As previously stated, gains between scenarios remained constant. The first flight parameter of concern is that of airspeed, which is likely to change both directly and indirectly, as the aircraft speed is adjusted for weight, sensor requirements and efficiency, while small changes are to be expected due to variations in wind.

Figure 7a and b show the result when airspeed is increased to 100 km/h, with FOV Track Error shown for both cross wind conditions. It can be seen that the increase in velocity slightly improves the performance of the STT IBVS controller, which can be attributed to a greater influence of the approach velocity compensator. One downfall is minor oscillations as the aircraft attempts to reduce residual track error, although

after approximately 15 s the response has died down. One thing to note with the BTT controller is that the steady state FOV Track Error is effectively eliminated as not only the angle of attack required to maintain altitude is reduced but faster airspeed results in a smaller WCA, both reducing the steady state FOV Track Error.

The final parameter to be considered is that of altitude, another which is likely to vary both directly, to meet the requirements of a mission, and indirectly due to variations in terrain height. To test the performance, altitude was increased to 100 m, with results shown in Fig. 7c and d. From the image perspective, the increase in height effectively reduces the scale of features, with a 15 m offset resulting in a feature that appears closer to the FOV centre. Thus from the controller perspective, this requires small correction even though the same amount of cross track error exists. Flying into the wind, the response is desirable and the controller effectively brings the feature into the image center. Flying with the wind, the response is less favorable as the residual track error compensator provides too much compensation, with the aircraft taking over 20 s to converge. Gains in this instance could be modified to improve this

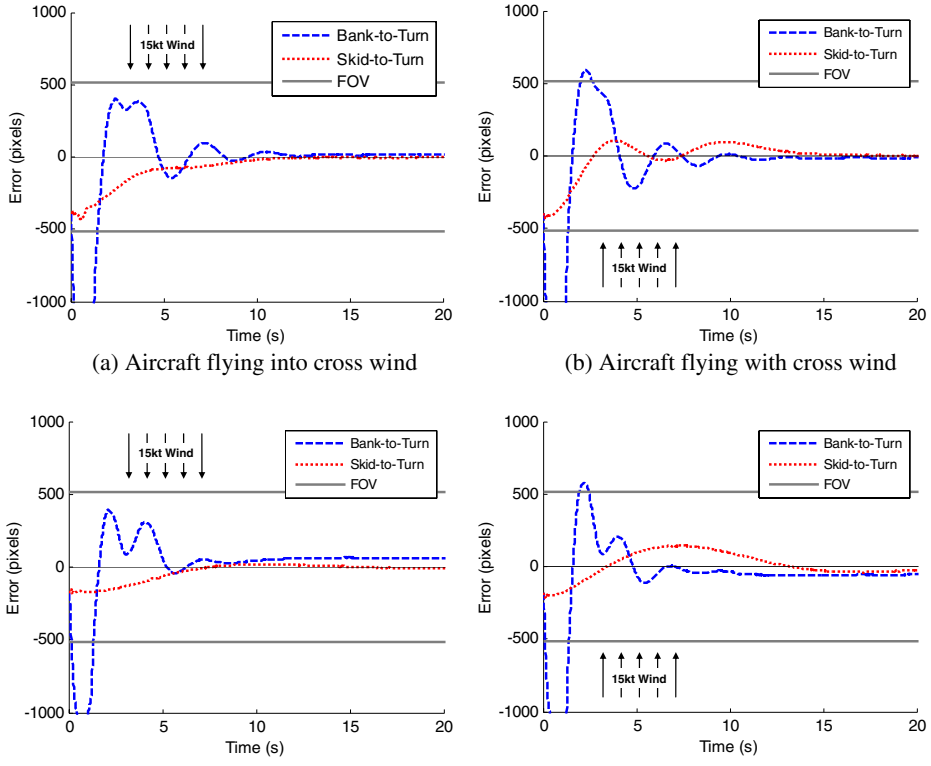

(a) Aircraft flying into cross wind

(b) Aircraft flying with cross wind

(c) Aircraft flying into cross wind

(d) Aircraft flying with cross wind

Fig. 7 Effect of increasing airspeed from 70 to 100 km/h (50 m altitude) (**a**, **b**), and altitude from 50 to 100 m (70 km/h) (**c**, **d**), with controllers using original gains. Results show track error as measured in the image plane as the aircraft flies into the wind to re-position (**a**, **c**) and with wind to re-position (**b**, **d**). Aircraft direction of travel is left to right, while *arrows* indicate direction of wind

response, although in practice it is unlikely that variations of this scale would be seen in a single flight.

5 Conclusion

This paper set out to highlight the benefits of Skid-to-Turn maneuvers over traditional Bank-to-Turn maneuvers for the tracking and inspection of locally linear infrastructure, and the importance of including visual feedback in control. Aside from the principal advantage of features remaining visible in the FOV of onboard body fixed sensors, STT maneuvers were shown to eliminate rotation that can lead to degraded data quality. Controller performance was demonstrated through a series of simulations with comparison to that of a BTT controller using GPS derived cross track error. The controller was also shown to be robust to variations in wind, airspeed and altitude with no modification to controller gains necessary over a range of flight parameters likely to be encountered.

From a practical point of view, the proposed controller should lend itself well to integration with operational UAVs, as the guidance controller is able to operate independent of any onboard autopilot. The addition of a suitable feature extraction algorithm to pre-process image data has not been addressed here, although will be necessary to close the overall control loop. In addition an interface between guidance controller and autopilot will be required to allow the IBVS controller to indicate when tracking is in progress and for the autopilot to hold altitude and airspeed while maintaining wings level flight. Future work will investigate controller robustness to errors in the feature extraction process, as well as tracking linear infrastructure through discontinous bends, as is present in powerlines and pipelines.

References

1. Campoy, P., Correa, J.F., Mondragon, I., Martinez, X., Olivares, M., Mejas, L., Artieda, J.: Computer vision onboard uavs for civilian tasks. J. Intell. Robot. Syst. **52**(3), 1–31 (2008)
2. Corke, P.I.: Visual control of robot manipulators—a review. In: Visual Servoing—Real-Time Control of Robot Manipulators Based on Visual Sensory Feedback. World Scientific, Singapore (1993)
3. Egbert, J., Beard, R.W.: Low altitude road following constraints using strap-down EO cameras on miniature air vehicles. In: Proceedings of the 2007 American Control Conference, New York City, USA. IEEE (2007)
4. Frew, E.W.: Comparison of lateral controllers for following linear structures using computer vision. In: Proceedings of the 2006 American Control Conference, Minneapolis, Minnesota, USA. IEEE (2006)
5. Holt, R.S., Beard, R.W.: Vision based road-following using proportional navigation. J. Intell. Robot. Syst. **57**(1), 193–216 (2010). doi:10.1007/s10846-009-9353-7
6. Mahony, R., Hamel, T.: Image based visual servo control of aerial robotic systems using linear image features. IEEE Trans. Robot. Autom. **21**(2), 227–239 (2005)
7. Mikhail, E.M., Bethel, J.S., McGlone, J.C.: Introduction to Modern Photogrammetry. Wiley, New York (2001)
8. Morris, S., Jones, H.: Examples of Commercial Applications Using Small UAVs, 20–23 September 2004
9. Niculescu, M.: Lateral track control law for Aerosonde UAV. In: 39th AIAA Aerospace Sciences Meeting and Exhibit. Reno, NV. American Institure of Aeronautics and Astronautics (2001)
10. Rathinam, S., Kim, Z.W., Sengupta, R.: Vision-based monitoring of locally linear structures using an unmanned aerial vehicle. J. Infrastruct. Syst. **14**(1), 52–63 (2008)

11. Rysdyk, R.: UAV Path Following for Constant Line-of-Sight, 15–18 September 2003
12. Stolle, S., Rysdyk, R.: Flight path following guidance for unmanned air vehicles with pan-tilt camera for target observation. In: 22nd Digital Avionics Systems Conference, vol. 2, pp. 8.B.3–81–12. IEEE (2003)
13. Wolf, P.R., Dewitt, B.A.: Elements of Photogrammetry: With Applications in GIS, 3rd edn. McGraw-Hill, Boston (2000)
14. Yokoyama, N., Ochi, Y.: Path planning algorithms for Skid-to-Turn Unmanned Aerial Vehicles. J. Guid. Control Dyn. **32**(5), 1531–1543 (2009)